

Hydrodynamic source with continuous emission in Au+Au collisions at $\sqrt{s} = 200$ GeV.

M.S. Borysova¹, Yu.M. Sinyukov², S.V. Akkelin², B. Erazmus³, Iu.A. Karpenko^{1,2}

December 14, 2018

Abstract

We analyze single particle momentum spectra and interferometry radii in central RHIC Au+Au collisions within hydro-inspired parametrization accounting for continuous hadron emission through the whole lifetime of hydrodynamically expanding fireball. We found that satisfactory description of the data is achieved for physically reasonable set of parameters if fairly long emission (~ 9 fm/c) from non space-like sectors of enclosed freeze-out hypersurface is taken into account. This protracted surface emission is compensated in outward interferometry radii by positive $r_{out} - t$ correlations that are the result of an intensive transverse expansion. The main features of the data are reproduced: in particular, the obtained ratio of the outward to sideward interferometry radii is less than unity and decreases when transverse momenta of pion pairs increase. The fitting temperature of emission from the surface of hydrodynamic tube approximately coincides with one found at chemical freeze-out in RHIC Au+Au collisions. A significant contribution of the surface emission to the spectra and correlation functions at relatively large transverse momenta that is found should be taken into account in advanced hydrodynamic models of ultrarelativistic nucleus-nucleus collisions.

¹ Taras Shevchenko National University, Kiev 01033, Volodymirs'ka 64, Ukraine.

² Bogolyubov Institute for Theoretical Physics, Kiev 03143, Metrologichna 14b, Ukraine.

³ SUBATECH, (UMR, Universite, Ecole des Mines, IN2P3/CNRS), 4, rue Alfred Castler, F-44070 Nantes Cedex 03, France.

PACS: 25.75.-q, 25.75.Gz, 25.75.Ld.

Keywords: *relativistic heavy ion collisions, HBT correlations, hydro-inspired parametrization.*

1 Introduction

Now there is common agreement that thermalized matter at unprecedented high energy density is created in relativistic heavy-ion collisions at RHIC [1]. The conclusion is based, in particular, on success of hydrodynamic models in description of measured single-particle hadron momentum spectra and elliptic flows [2]. This success gives, in principle, possibility to extract the equation of state (EoS) of the thermalized system and, then, provides insight into the high temperature phase transitions of strongly interacting matter formed in heavy ion collisions at RHIC.

However a quantitative determination of the EoS in hydrodynamic approach is a nontrivial problem: it depends on the initial conditions and "freeze-out" prescription. The later is necessary since one cannot use hydrodynamic equations till infinitely large times: then infinitesimally small final densities destroy the approximation of continuous medium of real particles. Usually, the freeze-out hypersurface which confines the 4-volume of hydrodynamic evolution is included as an external

input with respect to hydrodynamic equations. Then, typically, particle spectra are described by the Cooper-Frye prescription (CFp) [3] which treats freeze-out as a sudden transition from local thermal equilibrium to free streaming that happens on some space-like 3D hypersurface, e.g., on a space-like part of the isotherm: $T \simeq m_\pi$ [4].

However, a real process of freeze-out, or particle liberation, is quite complicated because the particles escape from the system during the whole period of its evolution (see, e.g., [5]). A method which is based on Boltzmann equation was recently proposed in Ref. [6] to describe spectra formation in hydrodynamic approach to A+A collisions using the escape probabilities. There and in Ref. [7] a region of applicability of CFp and its possible generalizations is discussed. In present work we do not consider the whole complexity of the freeze-out process (see, e.g., Refs. [6], [7], [8] and [9]). Instead we account for continuous in time emission process by applying the generalized Cooper-Frye prescription on *enclosed* freeze-out hypersurface. Such an enclosed hypersurface contains space-like sectors of the volume emission and non-space-like ones (with space-like vector of a normal) of the surface emission.

It is known for a long time [10] that the protracted surface emission may lead to the ratio of the outward to sideward interferometry radii, R_{out}/R_{side} , much larger than unity in typical scenarios of phase transition in heavy ion collisions [11]. These expectations are, however, in contrast to current experimental data from RHIC where $R_{out}/R_{side} \simeq 1$ (see, e.g., [12]). This discrepancy is a component of the so called "HBT puzzle" [13]. One might conclude then the duration of emission is very short and this could influent on a physical treatment of A+A collisions. However, R_{out}/R_{side} ratio is also quite sensitive to a form of freeze-out hypersurface, because, unlike R_{side} , R_{out} is a "mixture" of the "out" width, time spread of emission and the $r_{out} - t$ correlations. Indeed, in the Gaussian approximation for the correlation function the interferometry radii can be expressed in terms of the space-time variances (see, e.g., [14]):

$$R_i^2(p) = \langle (\Delta r_i - v_i \Delta t)^2 \rangle_p = \langle \Delta r_i^2 \rangle_p + v_i^2 \langle \Delta t^2 \rangle_p - 2v_i \langle \Delta r_i \Delta t \rangle_p, \quad (1)$$

where $v_i = p_i/p_0$, p_i , r_i ($i = out, side, long$) are the Cartesian components of the vectors \mathbf{v} , \mathbf{p} and \mathbf{r} respectively, and $p^\mu = (p_0, p_{out}, 0, p_{long})$ is the mean 4-momentum of the two registered particles. Here $\Delta r_i = r_i - \langle r_i \rangle_p$, $\Delta t = t - \langle t \rangle_p$, and $\langle \dots \rangle_p$ denotes the averaged (by means of distribution function) value taken at some momentum p . Note that $p_{side} = 0$ in the Bertsch-Pratt frame and therefore $p_{out} = p_T$, where p_T is the absolute value of transverse component of the vector \mathbf{p} . It is easy to see from Eq. (1) that *positive* $r_{out} - t$ correlations, $\langle \Delta r_{out} \Delta t \rangle_p > 0$, give a *negative* contribution to R_{out} reducing thereby the R_{out}/R_{side} ratio.¹ Therefore one can conclude that relatively small $R_{out}/R_{side} \simeq 1$ ratio in a case of a long time surface emission can take place if there are positive $r_{out} - t$ correlations in the corresponding sector of the freeze-out hypersurface. Such a sector has typically a space-like 4-vector of normal: then the interval between space-time points in such a sector can be, generally, space-like as well as time-like. While a bulk of hadrons are emitted from the sector with time-like normal (volume emission), the surface emission from the sector with the space-like normal can be, nevertheless, important for spectra and HBT radii formation (see the correspondent analysis in Ref. [16]), especially at relatively high p_T . A difference in temperatures and collective flows² in different freeze-out sectors can increase the effect and thus a consistent description of the single particle spectra and interferometry radii can be

¹This mechanism of reduction R_{out}/R_{side} ratio is realized in a multiphase transport (AMPT) model [15].

²It was found in Ref. [17] that the transport freeze-out process is similar to evaporation: high- p_T particles freeze-out early from the surface, while low- p_T ones decouple later from the system's center.

reached in hydrodynamically-motivated models with enclosed freeze-out hypersurface that accounts for continuous in time character of particles emission.

It is well known that when the freeze-out hypersurface σ has non-space-like sectors, the CFp is inconsistent because some particles will reenter the system. Then the CFp should be modified to exclude formally negative contributions to particle number at the corresponding momenta. The simple prescription that we will use here is to multiply distribution function on step θ - functions like $\theta(p_\mu n^\mu(x))$ [18, 19], $n^\mu n_\mu = \pm 1$, where n^μ is a time-like or space-like 4-vector normal to the freeze-out hypersurface σ and is directed away from the fluid.³ Thereby freeze-out is restricted to those particle for which $p_\mu n^\mu(x)$ is positive.

Sometimes, to avoid the above mentioned problems of CFp, the continuance of particles emission in heavy ion collisions is taken into account by means of the emission (source) function $S(x, p)$ (see, e.g., [14]) that is used instead of the distribution (Wigner) function $f(x, p)$ in some hydro-inspired parameterizations and is chosen usually to be proportional to the local equilibrium distribution function, $f_{l.eq}(x, p)$ with smearing (proper) time factor $\exp(-(\tau - \tau_0)^2 / \Delta\tau^2)$. First, such a prescription loses the extremely important information about $\tau - r_i$ correlations: it is naturally that at early times the emission function is concentrated mostly at the periphery of the system on the boundary with vacuum since particles cannot escape from a hot and dense central region. The approximation of the surface emission is, thus, much more realistic for the early times. Second, while the distribution function is well defined for a given state of the system, similar to the local Bose-Einstein or Fermi-Dirac distributions are associated with a locally equilibrated state, the $S(x, p)$ is much more complicated and model dependent [7, 20]. It is demonstrated in Ref. [6] basing on the particular exact solution of Boltzmann equation that the emission function is not proportional to the local equilibrium distribution (Wigner) function although the system is in the local equilibrium state. Therefore widely used (see, e.g., so called "blast wave" model [21]) "local-equilibrium" ansatz for $S \sim f_{l.eq.}$ is supported neither by analytic kinetic results nor numerical transport calculations except the formal case when all the particles are emitted simultaneously (the emission function then is proportional to delta function concentrated on freeze-out hypersurface). Perhaps, too large maximal collective velocities, closed to velocity of light, that are necessary to fit spectra in the blast-wave parametrization and a failure in fitting HBT radii (especially R_{side} , see Refs. [21]) are caused by improper description of the particle liberation process.

The aim of this work is a coherent description of pion, kaon and proton single particle momentum spectra as well as the HBT pion radii in central RHIC Au+Au collisions at $\sqrt{s_{NN}} = 200$ GeV by means of simple hydrodynamically-motivated parametrization with enclosed freeze-out hypersurface. As a matter of fact we generalize the blast-wave parametrization for a realistic case of continuous emission over the whole lifetime of fireball. We demonstrate that consistent description of the observables is possible if the freeze-out hypersurface has a non-space-like sector and a noticeable part of the particles are emitted from it.⁴ The later condition is satisfied when particles are emitted from the surface of expanding hydrodynamic tube soon after the hadronization which at early time happens at the periphery of the volume occupied by quark-gluon matter.

³If a fluid element that crosses the "time-like" sector of the freeze-out hypersurface decays preserving its total particle number, then the measure of integration is slightly different [18].

⁴An importance of the surface emission has been stressed also in Refs. [22] for opaque sources emitted particles from a surface layer of finite thickness, then $\langle \Delta r_{out}^2 \rangle_p < \langle \Delta r_{side}^2 \rangle_p$ reducing thereby R_{out}/R_{side} ratio.

2 Hydro-inspired parametrization of continuous hadronic freeze-out in central RHIC Au+Au collisions

We assume that particles are emitted from some 3D hypersurface when the fireball is in a locally equilibrated (leq) state,

$$f_i = f_{leq,i}(x, p) = (2\pi)^{-3} \left(\exp \left(\frac{u_\nu(x)p^\nu - \mu_i(x)}{T(x)} \right) \pm 1 \right)^{-1}, \quad (2)$$

characterized by the common temperature $T(x)$, collective velocity field $u_\mu(x)$ and for every particle species i by the chemical potentials $\mu_i(x)$. We refer the part of 3D hypersurface with the time-like normal vector as v - (volume) freeze-out, or final breakup, and the rest of the hypersurface with space-like normal vector as s - (surface) freeze-out corresponding to continuous emission prior to final breakup. We assume the particle densities are uniform at each v - and s - hypersurfaces separately, but, in general, are different between each other. Then the temperature and chemical potential fields are substituted in Eq. (2) by T_v , T_s and $\mu_{v,i}$, $\mu_{s,i}$ for v - and s -freeze-out respectively. For the sake of simplicity and to reduce the number of parameters we do not interpolate smoothly temperatures and chemical potentials between the "volume" and "surface" sectors of hypersurface. A longitudinally boost-invariant expansion is rather good approximation in mid-rapidity region at RHIC [23], therefore we assume the boost-invariance for longitudinal hydrodynamic velocities in this region, $v_L = z/t$, that allows us to parameterize t and $z \equiv r_{long}$ at 3D hypersurface σ by the form: $t_{v,s} = \tau_{v,s}(r) \cosh(\eta)$, $z_{v,s} = \tau_{v,s}(r) \sinh(\eta)$ in both sectors of the freeze-out hypersurface, where $\tau = \sqrt{t^2 - z^2}$ is the Bjorken proper time [24] and η is the longitudinal fluid rapidity, $\eta = \tanh^{-1} v_L$; in addition r is the absolute value of transverse coordinate $\mathbf{r}_T = (r \cos \phi, r \sin \phi)$. Taking into account also the transverse velocity component $v(r, \tau)$ in the longitudinally co-moving system, we obtain for the collective 4-velocity

$$u_{v,s}^\mu(r, \eta) = (\cosh \eta \cosh \eta_T^{v,s}, \sinh \eta_T^{v,s} \cos \phi, \sinh \eta_T^{v,s} \sin \phi, \sinh \eta \cosh \eta_T^{v,s}), \quad (3)$$

where $\eta_T^{v,s}(r, \tau_{v,s})$ is transverse fluid rapidity, $\eta_T = \tanh^{-1} v(r, \tau)$. The particle 4-momentum can be expressed through the momentum rapidity y , transverse momentum \mathbf{p}_T and transverse mass $m_T = \sqrt{m^2 + p_T^2}$,

$$p^\mu = (m_T \cosh y, \mathbf{p}_T, m_T \sinh y). \quad (4)$$

Then

$$\frac{p_\mu u^\mu}{T} = \frac{m_T}{T} \cosh(y - \eta) \cosh \eta_T - \frac{\mathbf{p}_T \cdot \mathbf{r}_T}{T r} \sinh \eta_T. \quad (5)$$

The "volume" and "surface" elements of the freeze-out hypersurface $\sigma(x)$ take the form

$$d\sigma_\mu^{v,s} = n_\mu^{v,s} d\sigma = \pm \tau_{v,s}(r) d\eta dr_x dr_y (\cosh \eta, -d\tau_{v,s}/dr_x, -d\tau_{v,s}/dr_y, -\sinh \eta), \quad (6)$$

where

$$n_\mu^{v,s} = \pm \frac{(\cosh \eta, -d\tau_{v,s}/dr_x, -d\tau_{v,s}/dr_y, -\sinh \eta)}{(\pm(1 - (d\tau_{v,s}/dr_x)^2 - (d\tau_{v,s}/dr_y)^2))^{1/2}}. \quad (7)$$

and "+" and "-" correspond to the v - and s - sectors of the hypersurface respectively. The surface "moves" outwards with velocity less than the velocity of light, $|dr_s(\tau)/d\tau| < 1$, then $|d\tau_s(r)/dr| > 1$. At the s -sector of the freeze-out hypersurface σ $d\tau_s/dr_x, d\tau_s/dr_y > 0$, therefore the product $p^\mu n_\mu$

will be negative if p_T is sufficiently small. If it is the case then such a particles do not really escape away from the system. For the particles with high transverse momenta $p^\mu n_\mu > 0$ and they are emitted from the surface of the system, practically, into vacuum streaming freely into detectors. To take this into account we use the modified Cooper-Frye prescription with the substitution [18, 19]

$$f_{l.eq.}(x, p) \rightarrow \theta(p_\mu n^\mu(x)) f_{l.eq.}(x, p) \quad (8)$$

to get single particle spectra $p_0 d^3 N / d^3 p$ for diverse particle species and the correlation function of pions $C(p, q)$:

$$p_0 \frac{d^3 N}{d^3 p} = \int p^\mu d\sigma_\mu \theta(p_\mu n^\mu(x)) f_{l.eq.}(x, p) \quad (9)$$

$$C(p, q) = 1 + \frac{|\int p^\mu d\sigma_\mu \theta(p_\mu n^\mu(x)) f_{l.eq.}(x, p) \exp(iqx)|^2}{(\int p_1^\mu d\sigma_\mu \theta(p_1^\mu n_\mu(x)) f_{l.eq.}(x, p)) (\int p_2^\mu d\sigma_\mu \theta(p_2^\mu n_\mu(x)) f_{l.eq.}(x, p))}. \quad (10)$$

Here $p = (p_1 + p_2)/2$, $q = p_1 - p_2$. To calculate the correlation function in the region of correlation peak we utilize smoothness mass shell approximation:

$$C(p, q) \approx 1 + \frac{|\int p^{*\mu} d\sigma_\mu \theta(p_\mu^* n^\mu(x)) f_{l.eq.}(x, p^*) \exp(iqx)|^2}{(\int p^{*\mu} d\sigma_\mu \theta(p^{*\mu} n_\mu(x)) f_{l.eq.}(x, p^*))^2} \quad (11)$$

where $p^{*\mu} = (\sqrt{m^2 + (\frac{\mathbf{p}_1 + \mathbf{p}_2}{2})^2}, \frac{\mathbf{p}_1 + \mathbf{p}_2}{2})$.

We assume that the source of particles in central Au + Au RHIC collisions has cylindrical symmetry and is strongly stretched out in the beam direction (*long*— direction): the longitudinal size is much larger than the corresponding length of homogeneity [25] (see also [26]). The latter allows us to neglect finiteness of the system in longitudinal direction when we calculate particle spectra in mid-rapidity region near $y \approx 0$. As for transverse direction we assume that source has a finite geometrical size encoded in the limits of integration over r : $0 < r < R_f$ for v —emission and $R_i < r < R_f$ for s —emission, where R_i and R_f are the initial and finite effective radii of the system.

To specify the model one needs to define $\tau(r)$ and transverse rapidity $\eta_T(r)$. We choose the simplest ansatz for ones aiming to catch the main features of particles emission. We assume that the volume (space-like) emission happens as supposed in the blast-wave model at the constant $\tau_v(r) = \tau_f$, and the surface emission takes place during the whole time of hydrodynamic evolution of system: $\tau_i < \tau_s < \tau_f$, where τ_i is the initial time of thermalization. Because the fireballs formed in RHIC collisions expand in transverse direction with rather high transverse velocity, we can assume that $d\tau_s(r)/dr > 0$ for "surface" freeze-out.⁵ For the sake of simplicity we parameterize $\tau_s(r)$ by linear function,

$$\tau_s(r) = a \cdot r + b. \quad (12)$$

Taking into account that $\tau_s(R_i) = \tau_i$ and $\tau_s(R_f) = \tau_f$ where R_i and R_f are the initial and final transverse radii respectively, $R_i < R_f$, we obtain that

$$a = \frac{\tau_f - \tau_i}{R_f - R_i}, \quad (13)$$

$$b = \tau_i - \frac{\tau_f - \tau_i}{R_f - R_i} R_i. \quad (14)$$

⁵This is in full correspondence with the form of hypersurface of constant densities (particle number and energy) in analytic ellipsoidal solutions of relativistic hydrodynamics [27].

The chosen form of freeze-out $\tau(r)$ is presented in the Fig. 1. It is convenient to parameterize "volume" as well as "surface" sector of 3D hypersurface by \mathbf{r}_T and longitudinal rapidity η , therefore the integration in Eqs. (9), (11) is carried out separately for "volume" and "surface" sectors: $\int d\sigma_\mu[\dots] \rightarrow \int d\sigma_\mu^v[\dots]_v + \int d\sigma_\mu^s[\dots]_s$.

To specify the transverse rapidity $\eta_T(r)$ we, first, tail smoothly the values of transverse rapidity in "volume" and "surface" sectors of hypersurface on their "border". Second, since a linear dependence of radial velocity profile on r was found in hydrodynamic simulations [28] for small transverse collective velocities $v \approx \eta_T$ near the center of the system at fixed τ , we assume that transverse flow rapidity profile depends linearly on r for "volume" freeze-out at $\tau = \tau_f$,

$$\eta_T^v(r, \tau_f) = \eta_T^{max} \frac{r}{R_f}, \quad (15)$$

where η_T^{max} is maximal transverse rapidity of fluid. As for the transverse rapidity profile in the "surface" sector of freeze-out hypersurface, we analyzed simplest parametrization with zero and non-zero transverse rapidity at the initial time τ_i . Fittings of the data privilege a non-zero initial transverse velocity that do not contradict to approximate linearly with radius of rapidity profile also at early times, in particular at τ_i . One of the simplest parameterizations that satisfied to this properties and allows us tail smoothly the values of transverse rapidity in the "volume" and "surface" sectors is the following transverse rapidity distribution:

$$\eta_T^s(r, \tau_s(r)) = \frac{\eta_T^{max}}{R_f} \frac{\sqrt{(\tau_s(r) - \tau_i)^2 + r^2}}{\sqrt{(\tau_f - \tau_i)^2 + r^2}}. \quad (16)$$

Note that $\tau_s(R_f) = \tau_f$ and $\eta_T^s(R_f, \tau_s(R_f)) = \eta_T^v(R_f, \tau_f) = \eta_T^{max}$.

Now the model is specified. In the next Section we apply the model developed to description of mid-rapidity pion, proton and kaon transverse momentum spectra and pion interferometry radii in RHIC Au+Au central collisions at $\sqrt{s_{NN}} = 200$ GeV.

3 Results and discussion

We assume the common enclosed freeze-out hypersurface for all the particles we are interested in: pions, kaons and protons. Then the model contains 7 parameters which are independent on species of the particles: τ_i , τ_f , R_i , R_f , T_v , T_s , η_T^{max} . As typically accepted, we suppose that at $\tau_i = 1$ fm/c the system is already in local thermal equilibrium and so will not consider this value as a free parameter. The chemical potentials $\mu_{s,j}$ that are different for diverse particle species j : negative pions, negative kaons and protons, are not fully free and their values are chosen to be closed to the results based on an analysis of particle number ratios. The reason is that a preliminary analysis shown a good fit for spectra and correlations formed on enclosed hypersurface cannot be reached if the "surface" temperature T_s is taken within standard range for kinetic freeze-out: $m_\pi \geq T_s \leq 100$ MeV, it should be taken higher then pion mass m_π . It forces us to conclude that the temperature of the surface emission is closed to the chemical freeze-out temperature or hadronization one, if chemical freeze-out happens at about the same time as is argued in Ref. [29]. Since a periphery of expanding system is less dense, the matter there is in the hadronic phase and hadrons can easily escape from this layer into surrounding vacuum despite relatively high temperature; this was argued in detail in Ref. [18]. This natural picture of the surface emission at the earlier times $\tau_s < \tau_f$ gives us possibility to fix $\mu_s = 0$ for pions and kaons, accounting for chemical equilibrium

of pions at chemical freeze-out and almost zero net strangeness in central RHIC Au+Au collisions at the top energy. Then the result of free T_s parameter fit of pion and kaon spectra demonstrates that the best fit fixes T_s to the value 150 MeV, that is indeed very close to the chemical freeze-out temperature 157 ± 3 MeV obtained in Ref. [30]. This *a posteriorly* justifies our assumption. The best fit of protons is achieved at $\mu_{s,p} = 40$ MeV that is slightly more than found in Ref. [30] value $\mu_B = 28.2 \pm 3.6$ MeV for baryochemical potential. Concerning the values $\mu_{v,j}$, it is readily to see that they are not free parameters in the model, because they should be fixed by means of the measured correspondent rapidity densities, dN_j/dy .

In detail the situation is somewhat more complicated since resonance decays contribute to the particle spectra and interferometry radii [31]. About $1/2 \div 2/3$ of pions, kaons and protons comes from those decays after chemical freeze-out happens in high energy heavy ion collisions [32, 26]. The correspondent contribution to pion spectra and interferometry radii was estimated in Ref. [33] within the hydrodynamic model developed in [26]. According to the results of Ref. [33] resonance decays do not change significantly the slopes of the transverse pion spectra in the region of interest for kinetic freeze-out temperatures T_v and flows at RHIC collisions (the resonance emission from the surface is small since heavy resonances have small heat velocities to escape from the expanding system). As for the interferometry radii, the pions coming from decays of short-lived resonances enhance the pion interferometry radii, in particular in the region of small p_T . This contribution to the pion interferometry radii decreases with an increase of transverse momenta of the pairs and, as was found in Ref. [33], is smaller than $6 \div 14$ % for $p_T > 0.3$ GeV (see also [34]). Based on these studies, we neglect changing of slopes of particle transverse spectra due to decays of resonances and fit the pion interferometry radii starting from $m_T \simeq 0.3$ GeV where the resonance contributions are fairly small. Finally, to fix μ_v for thermal (primary) particles, one needs to know which part of measured particles are produced by resonances after thermal (kinetic) freeze-out. Such a problem is not fully solved until now and needs in further analysis. Since the main aim in this paper is to disclose the main features of the physical picture of particle emission in central RHIC Au+Au collisions rather than fine tuning of the parameters and perfect description of the data, we fit the shares of thermal (direct) pions within reasonable limits discussed above, our final choice is presented in last column of Table 1.

The best fit is obtained for parameters that are shown in Tables 1 and 2, we present there also the parameters that are kept invariable through the fit procedure. As one can see from Figs. 2 – 6 and Tables 1, 2, a good description of pion, proton and kaon single-particle transverse momentum spectra and pion interferometry radii is achieved in mid-rapidity region of central $\sqrt{s_{NN}} = 200$ GeV Au+Au collisions for physically reasonable set of parameters. The STAR collaboration data are presented for illustration, we did not fit these data because they are limited by relatively small p_T as compare to PHENIX data while the surface emission gives significant contribution in the region of high transverse momenta. It is noteworthy, that the best fit is achieved when the system already at $\tau_i = 1$ fm/c expands in transverse direction with collective velocity field that reaches at the system border (at $r = R_i$) the value $v(R_i, \tau_i) \approx 0.34$ c. It may indicate that a noticeable contribution into build up of transverse flows at RHIC energies is given in earlier then 1 fm/c possibly pre-thermal stages of evolution.

TABLE 1.

Model parameters from fits of Au+Au RHIC $\sqrt{s_{NN}} = 200$ GeV data on π^- , K^- and p single particle spectra and π^- HBT radii. The ratio of registered particle numbers to thermal (primary) ones (last column) as well as μ_s for pions and kaons were kept invariable through fit procedures.

	μ_v MeV	μ_s MeV	$\frac{dN^{reg}/dy}{dN^{th}/dy}$
π^-	53	0	2.2
K^-	45	0	2.2
p	280	40	3.5

TABLE 2.

Model parameters from fits of Au+Au RHIC $\sqrt{s_{NN}} = 200$ GeV data on π^- , K^- and p single particle spectra and π^- HBT radii. The τ_i was kept invariable through fit procedures.

	τ_i fm/c	τ_f fm/c	R_i fm	R_f fm	T_v MeV	T_s MeV	η_T^{max}
π^-, K^-, p	1	10	7	11.3	110	150	0.73

The solid lines in Figs. 2 – 6 demonstrate the fit according to our model and the dashed lines indicate the contributions to particle spectra and interferometry radii from "volume" freeze-out solely; the later corresponds, in fact, to blast-wave model calculations with our "volume" freeze-out parameters and $\Delta\tau = 0$. The experimental data are taken from Refs. [35, 36, 37]. The Boltzmann approximation of the distribution functions is used for the single particle spectra and interferometry radii calculations for all particle species. One can see from Fig. 2 that "surface" emission leads to an noticeable enhancement of the single particle momentum spectra in high p_T region, increasing thereby the inverse spectra slope, or effective temperature. This happens because the particles with relatively low p_T emitted from the "surface" part of freeze-out hypersurface may reenter the system and so their contribution to spectra is suppressed, while the particles with sufficiently high p_T are liberated freely. This effect is taken into account, as discussed in the previous Section, by multiplying the distribution functions on the step function, see Eq. (8), restricting thus the freeze-out to those particles for which the product $p^\mu n_\mu$ is positive. Note that in the blast-wave parametrization, that takes into account only "volume" emission, such a high effective temperature can be obtained only at the cost of very high transverse flow ($\eta_T^{max} \approx 0.9$ and so $v^{max} \approx 0.7$ c, while in our parametrization $\eta_T^{max} \approx 0.72$, $v^{max} \approx 0.6$ c) at freeze-out [21], that seems less realistic and is more difficult to reproduce in hydrodynamic models of the system evolution.

The Figs. 3 – 6 represent our results for the interferometry radii of negative pions. Note that the interferometry radii are measured by the PHENIX Collaboration for 0 – 30 % centrality events at $\sqrt{s_{NN}} = 200$ GeV [37]. Therefore, to adjust the results of PHENIX Collaboration to the most central 0 – 5 % centrality bin, we increase the corresponding interferometry radii by a factors calculated in accordance with N_{part} dependence of the Bertsch-Pratt radius parameters found in Ref. [37]. As one can see from Fig. 3, the interplay between (i) a long emission time, $\tau_f - \tau_i$, that gives an increase of the R_{out} radius, and (ii) the positive $r_{out} - t$ correlations at the "surface" part of hypersurface where $d\tau_s/dr > 0$, that reduces the radius, provides a *moderate* increase of R_{out} as compare with "volume" emission at constant τ .⁶ The R_{side} radius, see Fig. 4, is almost not affected by the "surface" emission.⁷ As to R_{long} , that is presented in Fig. 5, it is less than in the "volume" emission case. The reason is that R_{long} is strongly affected by the value of the emission time τ [25] and, thereby, is reduced by the emission from early times $\tau < \tau_f$. This can explain an apparently low freeze-out value of τ in relativistic heavy ion collisions if it is extracted supposing instantaneous "volume" emission at constant τ .

⁶The conclusion that long-lived fireball can be compatible with HBT measurements is made also in Ref. [38]

⁷An independence of R_{side} on transport opacity was also found in covariant transport model [17].

The Fig. 6 represents our result for R_{out}/R_{side} ratio. One can see that the "volume" blast-wave like emission (at a constant τ) leads to a rather low R_{out}/R_{side} ratio and, thereby, underestimates this quantity essentially. The "extra"- reduction of the value of R_{out} is typical for sharp freeze-out hypersurface with step density profile in out-direction, $n(r) \sim \theta(R - r_{out})$ and the maximal velocity on the edge. The same boundary effect of additional broadening of the correlation function at large momenta in the case of sharp freeze-out in long-direction have been found and described in detail in Ref. [39]. As one can see from Fig. 6 this effect becomes softer for enclosed freeze-out hypersurface despite the maximal velocity is also achieved at maximal transverse radius that system occupies during its evolution. However, the negative $t - r_{out}$ correlations can destroy the effect of relative reduction of R_{out} at all. That is why the positive $t - r_{out}$ correlations in our model are very important to achieve the satisfactory description of the experimental data.

4 Summary

We have studied the effect of long time particle emission on particle spectra and interferometry radii basing on the hydro-inspired parametrization of enclosed freeze-out hypersurface and distribution functions. As a matter of fact our model generalizes the "blast-wave" parametrization, that has difficulties in a fitting of the HBT radii and results in too large transverse velocities. We demonstrate that Au+Au RHIC $\sqrt{s_{NN}} = 200$ GeV data on π^- , K^- and p single particle spectra and π^- interferometry radii can be described by physically reasonable set of parameters if rather protracted emission (~ 9 fm/c) from the "surface sector" of the hypersurface that "moves" outward is taken into account. The phase-space distribution of particles emitted from the surface prior to the fireball breakup is similar to the local chemical equilibrium distribution with parameters that are rather close to ones found at chemical freeze-out in RHIC Au+Au collisions. This could be a signature of the transformation of quark-gluon matter to hadron gas at the periphery of the system with subsequent hadronic emission just after such a transition from the boundary of the fireball during the whole time of system's hydro evolution.

Thereby, the simple physical arguments requiring the freeze-out hypersurface to be enclosed for finite expanding systems result in successful description of hadronic spectra and interferometry radii. It means the particle emission from the early stages of fireball evolution has to be taken into account in advanced hydrodynamic models of A+A collisions.⁸ A quantitative description of continuous particle escaping can be done, in particular, within the hydro-kinetic approach to spectra formation proposed in Ref. [6].

Acknowledgments

The research described in this publication was made possible in part by Award No. UKP1-2613-KV-04 of the U.S. Civilian Research & Development Foundation for the Independent States of the Former Soviet Union (CRDF). Research carried out within the scope of the ERG (GDRE): Heavy ions at ultrarelativistic energies - a European Research Group comprising IN2P3/CNRS, Ecole des Mines de Nantes, Universite de Nantes, Warsaw University of Technology, JINR Dubna, ITEP Moscow and Bogolyubov Institute for Theoretical Physics NAS of Ukraine. The work was also supported by NATO Collaborative Linkage Grant No. PST.CLG.980086.

⁸The back reaction of evaporation of particles off the surface of the system created on the fluid dynamics was studied within boost-invariant hydrodynamics in Ref. [40].

References

- [1] RHIC Collaboration white papers: I. Arsene *et al.* (The BRAHMS Collaboration), Nucl. Phys. A **757**, 1 (2005); B.B. Back *et al.* (The PHOBOS Collaboration), Nucl. Phys. A **757**, 28 (2005); J.Adams *et al.* (The STAR Collaboration), Nucl. Phys. A **757**, 102 (2005); K. Adcox *et al.* (The PHENIX Collaboration), Nucl. Phys. A **757**, 184 (2005).
- [2] U. Heinz, J. Phys. G **31**, S717 (2005); arXiv: nucl-th/0504011.
- [3] F. Cooper, G. Frye, Phys. Rev. D **10**, 186 (1974).
- [4] L.D. Landau, Izv. Akad. Nauk SSSR, Ser. Fiz. **17**, 51 (1953).
- [5] L.V. Bravina, K. Tywoniuk, E.E. Zabrodin, J. Phys. G **31**, S989 (2005).
- [6] Yu.M. Sinyukov, S.V. Akkelin, Y. Hama, Phys. Rev. Lett. **89**, 052301 (2002).
- [7] S.V. Akkelin, M.S. Borysova, Yu.M. Sinyukov, Acta Phys. Hung. A **22**, 165 (2005).
- [8] K.A. Bugaev, Phys. Rev. C **70**, 034903 (2004).
- [9] L.P. Csernai, V.K. Magas, E. Molnar, A. Nyiri, K. Tamosiunas, arXiv: hep-ph/0505228.
- [10] S. Pratt, Phys. Rev. D **33**, 1314 (1986); Phys. Rev. C **49**, 2722 (1994).
- [11] G.F. Bertsch, Nucl. Phys. A **498**, 173 (1989); D.H. Rischke, M. Gyulassy, Nucl. Phys. A **608**, 479 (1996); S. Soff, S.A. Bass, A. Dumitru, Phys. Rev. Lett. **86**, 3981 (2001); S. Soff, S.A. Bass, D.H. Hardtke, S.Y. Panitkin, Phys. Rev. Lett. **88**, 072301 (2002).
- [12] H. Appelshauser, J. Phys. G **30**, S935 (2004); D. Magestro, J. Phys. G **31**, 265 (2005).
- [13] U. Heinz, Nucl. Phys. A **721**, 30 (2003); M. Lisa, S. Pratt, R. Soltz, U. Wiedemann, arXiv: nucl-ex/0505014.
- [14] U.A. Wiedemann, U. Heinz, Phys. Rep. **319**, 145 (1999).
- [15] Z.W. Lin, C.M. Ko, S. Pal, Phys. Rev. Lett. **89**, 152301 (2002); Z.W. Lin, C.M. Ko, B.A. Li, B. Zhang, S. Pal, arXiv: nucl-th/0411110.
- [16] H. Heiselberg, Heavy Ion Phys. **5**, 435 (1997).
- [17] D. Molnar, M. Gyulassy, Phys. Rev. Lett. **92**, 052301 (2004).
- [18] Yu.M. Sinyukov, Z. Phys. C **43**, 401 (1989).
- [19] K.A. Bugaev, Nucl. Phys. A **606**, 559 (1996); Cs. Anderlik *et al.*, Phys. Rev. C **59**, 3309 (1999).
- [20] K. Zalewski, Acta Phys. Polon. B **34**, 3379 (2003).
- [21] F. Retiere, M. Lisa, Phys. Rev. C **70**, 044907 (2004); B. Tomasik, Nucl. Phys. A **749**, 209 (2005).

- [22] H. Heiselberg, A.P. Vischer, Eur. Phys. J. C **1**, 593 (1998); L. McLerran, S.S. Padula, arXiv: nucl-th/0205028; S.S. Padula, Nucl. Phys. A **715**, 637 (2003).
- [23] P.F. Kolb, U. Heinz, in Quark Gluon Plasma 3, eds. R.C. Hwa, X.N. Wang (World Scientific, Singapore, 2004), p. 634 [arXiv: nucl-th/0305084].
- [24] J.D. Bjorken, Phys. Rev. D **27**, 140 (1983).
- [25] A.N. Makhlin, Yu.M. Sinyukov, Z. Phys. C **39**, 69 (1988); Yu.M. Sinyukov, Nucl. Phys. A **498**, 151c (1989); S.V. Akkelin, Yu.M. Sinyukov, Phys. Lett. B **356**, 525 (1995); Z. Phys. C **72**, 501 (1996).
- [26] S.V. Akkelin, P. Braun-Munzinger, Yu.M. Sinyukov, Nucl. Phys. A **710**, 439 (2002).
- [27] Yu.M. Sinyukov, Iu.A. Karpenko, arXiv: nucl-th/0505041; arXiv: nucl-th/0506002.
- [28] P.F. Kolb, Heavy Ion Phys. **21**, 243 (2004).
- [29] P. Braun-Munzinger, J. Stachel, C. Wetterich, Phys. Lett. B **596**, 61 (2004).
- [30] M. Kaneta, N. Xu, arXiv: nucl-th/0405068.
- [31] M. Gyulassy, S.S. Padula, Phys. Lett. B **217**, 181 (1988).
- [32] P. Braun-Munzinger, J. Stachel, J.P. Wessels, N. Xu, Phys. Lett. B **344**, 43 (1995); Phys. Lett. B **365**, 1 (1996); P. Braun-Munzinger, I. Heppe, J. Stachel, Phys. Lett. B **465**, 15 (1999); P. Braun-Munzinger, D. Magestro, K. Redlich, J. Stachel, Phys. Lett. B **518**, 41 (2001); P. Braun-Munzinger, K. Redlich, J. Stachel, in Quark Gluon Plasma 3, eds. R.C. Hwa, X.N. Wang (World Scientific, Singapore, 2004), p.491 [arXiv: nucl-th/0304013].
- [33] S.V. Akkelin, Yu.M. Sinyukov, Phys. Rev. C **70**, 064901 (2004).
- [34] U. Wiedemann, U. Heinz, Phys. Rev. C **56**, 3256 (1997).
- [35] S.S. Adler *et al.* (The PHENIX Collaboration), Phys. Rev. C **69**, 034909 (2004).
- [36] J. Adams *et al.* (The STAR Collaboration), Phys. Rev. Lett. **92**, 112301 (2004); J. Adams *et al.* (The STAR Collaboration), Phys. Rev. C **71**, 044906 (2005).
- [37] S.S. Adler *et al.* (The PHENIX Collaboration), Phys. Rev. Lett. **93**, 152302 (2004).
- [38] T. Renk, Phys. Rev. C **69**, 044902 (2004).
- [39] V.A. Averchenkov, A.N. Makhlin, Yu.M. Sinyukov, Sov. J. Nucl. Phys. **46**, 905 (1987); Yad. Fiz. **46**, 1525 (1987).
- [40] A. Dumitry, C. Spieles, H. Stöcker, C. Greiner, Phys. Rev. C **56**, 2202 (1997).

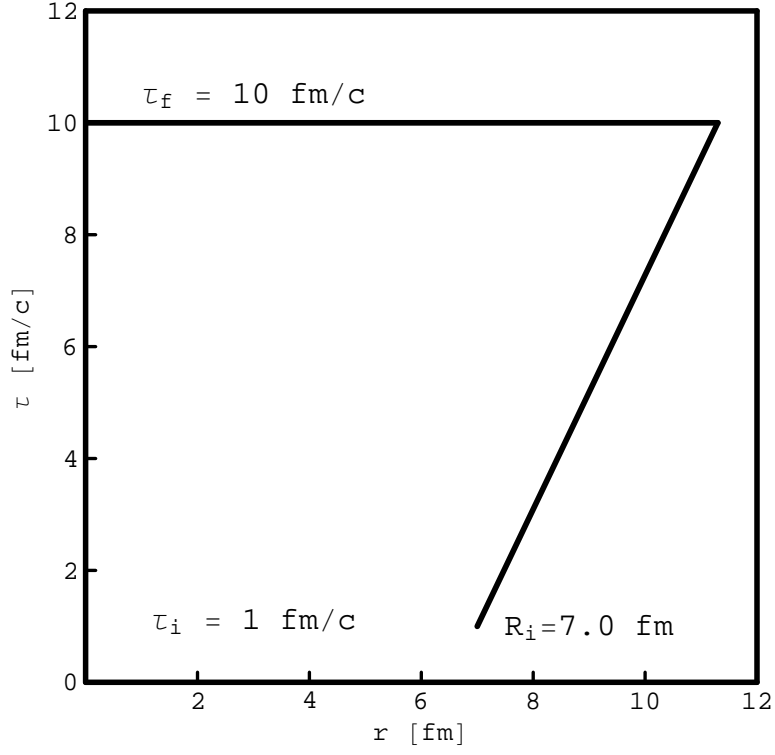


Figure 1: The enclosed freeze-out hypersurface $\tau(r)$. See the text for detail.

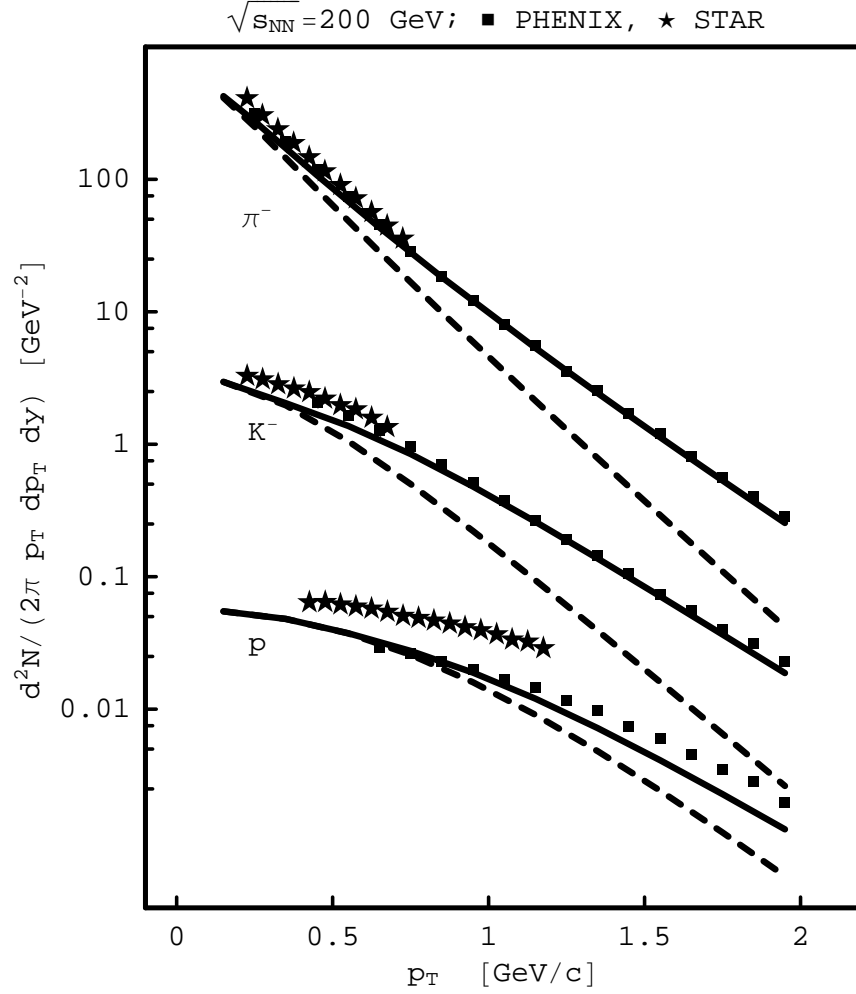


Figure 2: Comparison of the single-particle momentum spectra measured by the PHENIX Collaboration with the model calculations performed for whole enclosed hypersurface (solid lines) and for shelf-like part, see Fig. 1, solely (dashed lines). For convenience of plots location the measured p spectra are reduced in 100 times and K^- spectra in 8 times. The STAR data are not fitted and are presented for illustration.

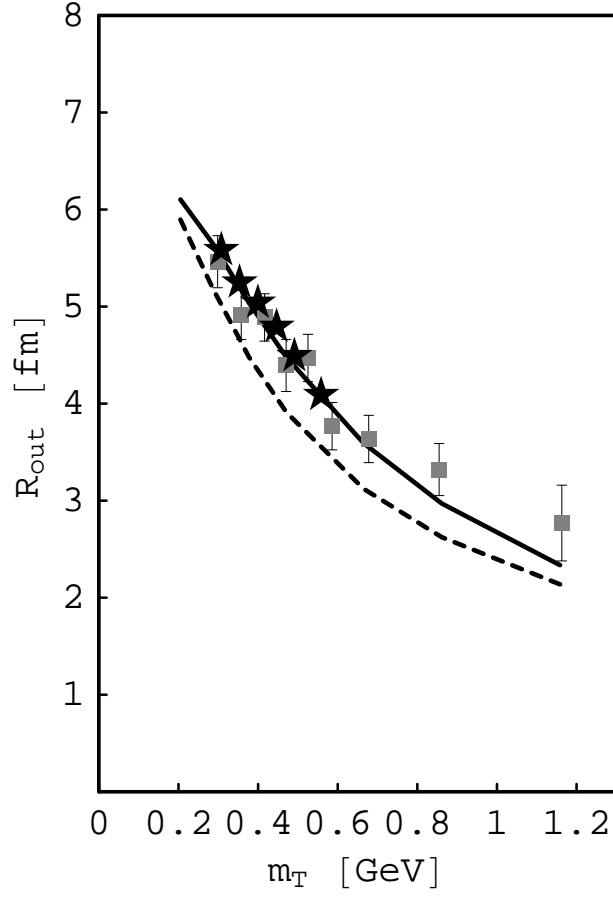


Figure 3: Comparison of the pion source R_{out} radii measured by the STAR (stars) and PHENIX (boxes) Collaborations with model calculations performed for whole enclosed hypersurface (solid line) and for shelf-like part only (dashed line). The PHENIX data are adjusted for most central bin (see the text for detail).

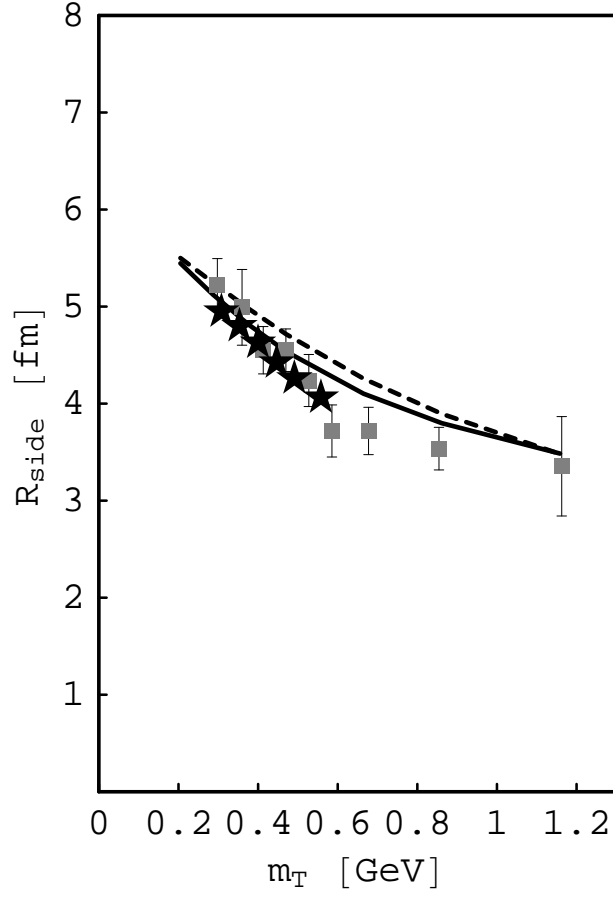


Figure 4: Comparison of the pion source R_{side} radii measured by the STAR (stars) and PHENIX (boxes) Collaborations with model calculations performed for whole enclosed hypersurface (solid line) and for shelf-like part only (dashed line). The PHENIX data are adjusted for most central bin (see the text for detail).

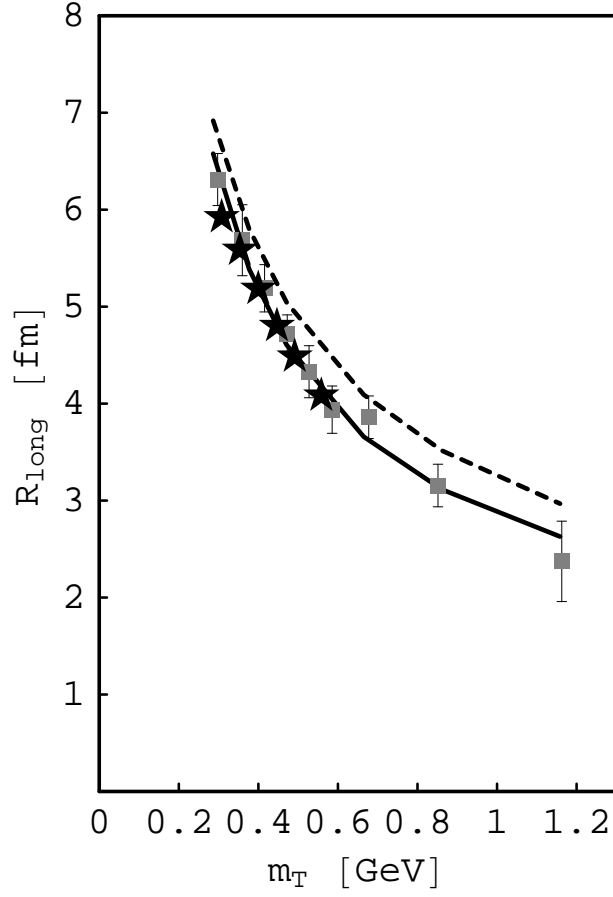


Figure 5: Comparison of the pion source R_{long} radii measured by the STAR (stars) and PHENIX (boxes) Collaborations with model calculations performed for whole enclosed hypersurface (solid line) and for shelf-like part only (dashed line). The PHENIX data are adjusted for most central bin (see the text for detail).

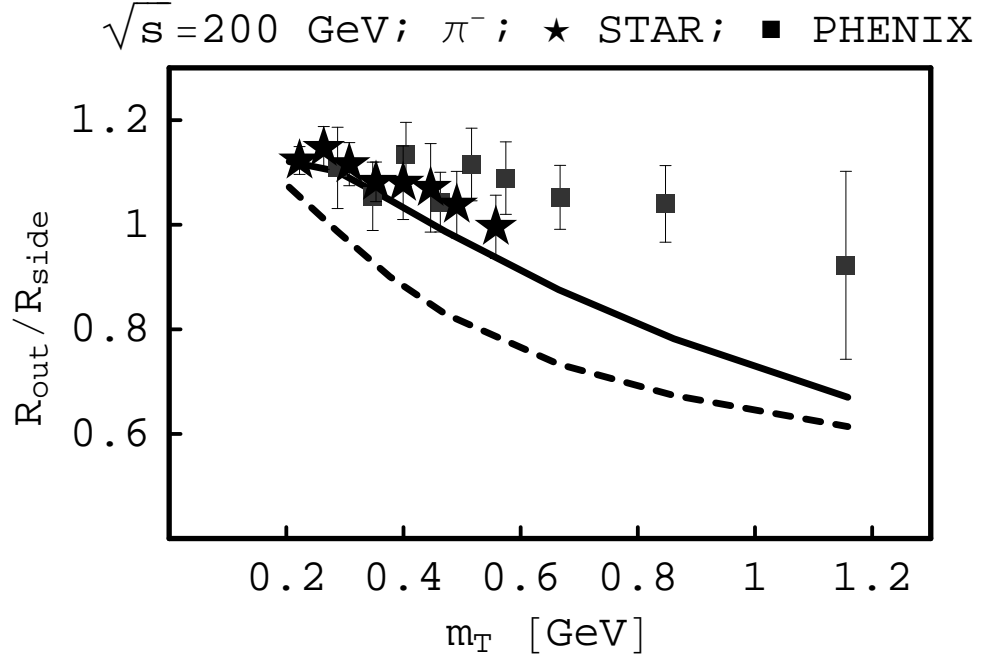


Figure 6: Comparison of the measured by the STAR (stars) and PHENIX (boxes) Collaborations pion R_{out}/R_{side} ratios with model calculations performed for whole enclosed hypersurface (solid line) and for shelf-like part only (dashed line).